Talanta 122 (2014) 272–277

Contents lists available at ScienceDirect

Talanta

journal homepage: www.elsevier.com/locate/talanta

A new rapid colorimetric detection method of Al^{3+} with high sensitivity and excellent selectivity based on a new mechanism of aggregation of smaller etched silver nanoparticles

Ningning Yang [a,b,1], Yuexia Gao [a,b,c,1], Yujie Zhang [a,b], Zheyu Shen [a,b,*], Aiguo Wu [a,b,*]

[a] Key Laboratory of Magnetic Materials and Devices, Ningbo Institute of Materials Technology & Engineering, Chinese Academy of Sciences, Ningbo, Zhejiang 315201, China
[b] Division of Functional Materials and Nano Devices, Ningbo Institute of Materials Technology & Engineering, Chinese Academy of Sciences, Ningbo, Zhejiang 315201, China
[c] The School of Materials Science and Chemical Engineering, Ningbo University, Ningbo 315211, China

ARTICLE INFO

Article history:
Received 4 November 2013
Received in revised form
7 January 2014
Accepted 11 January 2014
Available online 31 January 2014

Keywords:
Aluminum ions
Rapid colorimetric detection
High sensitivity
Excellent selectivity
Aggregation of smaller etched silver nanoparticles

ABSTRACT

As a pathogenic factor of the Alzheimer's disease, aluminum has been associated with the damage of the central nervous system in humans. In this study, we propose a new facile and rapid colorimetric detection method of Al^{3+} with excellent selectivity and high sensitivity based on silver nanoparticles (AgNPs) stabilized by reduced glutathione (GSH) in the presence of L-cysteine (Cys). The new mechanism of our Al^{3+} detection system based on GSH-AgNPs, i.e., aggregation of smaller etched GSH-AgNPs, are confirmed by TEM, EDS and DLS. The aggregation of smaller etched GSH-AgNPs results in obvious color change of the nanoparticle dispersion from yellow to reddish brown, and red shift and intensity decrease of the surface plasmon resonance (SPR) absorption. The GSH concentration, Cys concentration and pH value of the GSH-AgNPRs-based detection system are respectively optimized to be 10.0 mM, 50.0 mM and 6.0 according to the sensing effect of Al^{3+}. At the optimized conditions, the selectivity of the GSH-AgNPs detection system for Al^{3+} is excellent compared with other ions including K^+, Mg^{2+}, Fe^{3+}, Co^{2+}, Mn^{2+}, Zn^{2+}, Cd^{2+}, Pb^{2+}, Ca^{2+}, Ba^{2+}, Cu^{2+}, Cr^{3+}, Hg^{2+}, Ni^{2+}, $Cr_2O_7^{2-}$, SO_4^{2-}, $C_2O_4^{2-}$, PO_4^{3-} and CO_3^{2-}. Furthermore, this detection system is very sensitive for Al^{3+}. The limit of detection (LOD) is 1.2 μM by the naked eyes and 0.16 μM by UV–vis spectra, which are both much lower than the national drinking water standards (7.4 μM). Furthermore, the UV–vis detection offers a good linear detection range from 0.4 to 4.0 μM (R^2=0.9924), which indicates that our developed detection system can also be used for the quantitative analysis of Al^{3+}. The detection results of real water samples indicate that this method can be used for real water detection.

1. Introduction

Aluminum is the third most abundant element in the Earth's crust. Aluminum and aluminum-containing products have been applied more and more often to human's daily lives, aerospace and other fields, due to its abundance, active chemical properties and excellent physical properties. Meanwhile, pollutions and diseases caused by aluminum and aluminum-containing products are increasing. Aluminum ion (Al^{3+}) is associated with many neurological diseases. It can reduce the activity of some enzymes, such as aconitase, allosteric enzyme, glutamate dehydrogenase, δ-aminolevulinic acid dehydratase, nitrate reductase, mannitol dehydrogenase and trehalase [1–5]. Research shows that Al^{3+} is a pathogenic factor of the Alzheimer's disease because Al^{3+} can induce oxidative stress in brain tissue [6–8].

Nowadays, traditional detection methods for Al^{3+} include flameless atomic absorption spectrophotometry, inductively coupled plasma atomic emission spectrometry (ICP-AES), inductively coupled plasma mass spectrometry (ICP-MS), electrothermal atomic absorption (ETAAS), neutron activation analysis (NAA), high performance liquid chromatography (HPLC) and fluorimetry [9–12]. Although these methods have high sensitivity and excellent selectivity, they are not suitable for on-site analysis because the sample pretreatments are complicated and the detection time is long.

In recent years, many colorimetric assay methods have been reported for detection of metal ions based on noble metal nanoparticles due to their high extinction coefficient and strong surface

* Corresponding authors at: Key Laboratory of Magnetic Materials and Devices, Ningbo Institute of Materials Technology & Engineering, Chinese Academy of Sciences, Ningbo, Zhejiang 315201, China.
Tel.: +86 574 86685039, +86 574 87617278; fax: +86 574 86685163.
E-mail addresses: shenzheyu@nimte.ac.cn (Z. Shen), aiguo@nimte.ac.cn (A. Wu).
[1] Both authors contributed equally for this work.

0039-9140/$ - see front matter © 2014 Elsevier B.V. All rights reserved.
http://dx.doi.org/10.1016/j.talanta.2014.01.035

plasmon resonance (SPR) properties [13–22]. To date, however, only three Al^{3+} colorimetric detection systems based on noble metal nanoparticles, which are introduced below, are reported [23–25]. Li et al. presented a colorimetric assay method based on pentapeptide modified gold nanoparticles for selective detection of Al^{3+} both in aqueous solution and on living cellular surfaces [23]. The limit of detection (LOD) is 0.2 μM by UV–vis spectrum. Because Al^{3+} cannot be detected by the naked eyes using this method, it is not applicable for on-site real-time detection. Zhang et al. proposed new Al^{3+} colorimetric detection systems based on mononucleotide-modified gold or silver nanoparticles [24], whose LOD is 3.0 μM or 1.5 μM by the naked eyes, and 0.46 μM or 0.09 μM by UV–vis spectrum. Although the LODs by the naked eyes or UV–vis spectrum are all lower than the national table-water standard (7.4 μM), the detection process is too complicated to be used for the on-site real-time detection because the gold or silver nanoparticle dispersions need to be centrifuged before Al^{3+} detection. Chen et al. reported a new colorimetric detection method of Al^{3+} based on citrate-capped gold nanoparticles [25]. The LOD is 1.0 μM by naked eyes, which is also lower than the national table-water standard. However, Cr^{3+} and some other trivalent cations have interference to the Al^{3+} detection. Therefore, it is necessary to develop a new rapid Al^{3+} colorimetric detection method with applicability for on-site real-time detection, excellent selectivity and high sensitivity.

In this study, we propose a new facile and rapid Al^{3+} colorimetric detection system with applicability for on-site real-time detection, excellent selectivity and high sensitivity based on silver nanoparticles (AgNPs) stabilized by reduced glutathione (GSH) in the presence of L-cysteine (Cys). The proposed new mechanism for Al^{3+} detection, i.e., aggregation of smaller etched AgNPs, is shown in Scheme 1. As a stabilizer, GSH molecule can be absorbed onto the surface of AgNPs via the thiol group. However, Cys (another smaller molecule containing a thiol group) may attack the surface of the AgNPs and replace GSH to some extent. Slight aggregation of AgNPs may happen because Cys is worse than GSH as a stabilizer. Furthermore, Cys can etch the AgNPs because of the unique and strong interaction between the thiol groups and AgNPs [26] resulting in decrease of the nanoparticle size. Because Al^{3+} can form complex with GSH [27], the smaller GSH-AgNPs etched by Cys aggregate to a great extent after being incubated with Al^{3+}.

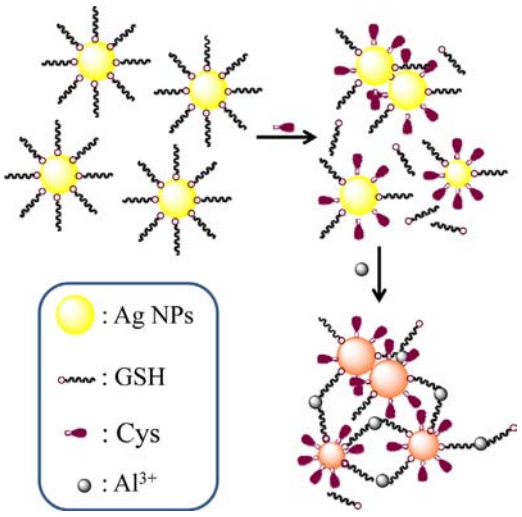

Scheme 1. Mechanism scheme of GSH-AgNPs with Cys for rapid colorimetric detection of Al^{3+}. Cys may attack the surface of the AgNPs and replace GSH to some extent. The size of the AgNPs decreases because AgNPs could be etched by Cys. Slight aggregation may also happen because Cys is worse than GSH as a stabilizer. The smaller GSH-AgNPs etched by Cys aggregate to a great extent after being incubated with Al^{3+}.

The severe aggregation of the smaller etched GSH-AgNPs results in obvious color change of the nanoparticle dispersion from yellow to reddish brown, and red shift and intensity decrease of the surface plasmon resonance (SPR) absorption. Due to the new mechanism of aggregation of smaller etched AgNPs, our GSH-AgNPs-based detection system is very sensitive for Al^{3+}. The LOD is 1.2 μM by the naked eyes and 0.16 μM by UV–vis spectra. Furthermore, the selectivity of this Al^{3+} detection system is excellent compared with other metal ions and anions including K^+, Mg^{2+}, Fe^{3+}, Co^{2+}, Mn^{2+}, Zn^{2+}, Cd^{2+}, Pb^{2+}, Ca^{2+}, Ba^{2+}, Cu^{2+}, Cr^{3+}, Hg^{2+}, Ni^{2+}, $Cr_2O_7^{2-}$, SO_4^{2-}, $C_2O_4^{2-}$, PO_4^{3-} and CO_3^{2-}.

2. Experimental

2.1. Materials and characterization

Analytical grade reagents, such as reduced GSH, $AgNO_3$, sodium borohydride ($NaBH_4$), Cys, NaOH, HCl, KCl, $MgCl_2$, $FeCl_3$, $CoCl_2$, $MnCl_2$, $ZnCl_2$, $CdCl_2$, $PbCl_2$, $CaCl_2$, $BaCl_2$, $CuCl_2$, $CrCl_3$, $HgCl_2$, $NiCl_2$, $AlCl_3$, $K_2Cr_2O_7$, Na_2SO_4, $Na_2C_2O_4$, Na_2S, Na_3PO_4 and Na_2CO_3, were all obtained from Sinopharm Chemical Reagent Co. Ltd. All the chemicals were used as received. Transmission electron microscopy (TEM) was performed using a Tecnai F20 instrument operated at 200 kV. The samples were directly loaded onto the copper grid for TEM observation. UV–vis spectroscopy was performed using a T10CS instrument from Beijing Purkinje General Instrument Co., Ltd. Size distribution of GSH-stabilized AgNPs (GSH-AgNPs) was measured by a DLS zetasizer (Nano ZS, Malvern Instruments Ltd.). The Al^{3+} concentrations in real water samples were detected by Inductively coupled plasma mass spectrometry (ICP-MS, Perkin Elmer) as controls. MilliQ water was used for all experiments.

2.2. Preparation of GSH-AgNPs

GSH-AgNPs were prepared by a previously reported method with only minor modifications [28]. Typically, 2.0 mL 20.0 mM $AgNO_3$ was added into 187.6 mL Milli-Q water under stirring. After 10.0 min, 6.4 mL of freshly prepared $NaBH_4$ (0.1 M) aqueous solution was rapidly added under vigorous stirring. After addition of $NaBH_4$, the stirring speed was turned down to a facile speed. After 5.0 min, 4.0 mL of GSH aqueous solution (1.0 mM) was dropwise added and the reaction was kept for 2.0 h.

2.3. Detection of Al^{3+}

9.0 mL of the above GSH-AgNPs dispersion was mixed with 1.0 mL of Cys aqueous solution (0–150.0 mM) and 0.3 mL of GSH aqueous solution (0–20.0 mM). The pH value of the mixture was then tuned from 4.0 to 9.0 to form the final detection system. The final detection system was mixed with different concentration of Al^{3+} or other ions solution by the volume ratio of 4:1. One min later, the color change of the mixtures was observed and the corresponding UV–vis absorption was recorded with T10CS UV–vis spectrophotometer.

2.4. Detection of Al^{3+} in real water samples

The Al^{3+} in real water samples (tap water or lake water) was also detected by using standard addition method. Various concentrations of Al^{3+} was added into real water samples, which were used directly without purification, and detected by our Al^{3+} detection system. Typically, 200 μL of Al^{3+} aqueous solutions with different concentrations, which were prepared using MilliQ water, tap water or lake water, were respectively added into 800 μL of Cys

etched GSH-AgNP dispersions. 1 min later, the color change of the mixtures was observed and the corresponding UV–vis absorption was recorded with T10CS UV–vis spectrophotometer.

3. Results and discussion

3.1. Optimization of experimental conditions

The Cys concentration (in the 1.0 mL of Cys aqueous solution added into the GSH-AgNPs dispersion before Al^{3+} detection), GSH concentration (in the 0.3 mL of GSH aqueous solution added into the GSH-AgNPs dispersion before Al^{3+} detection) and pH value of the GSH-AgNPs-based detection system are optimized according to the sensing effect of Al^{3+}.

The GSH-AgNPs dispersion without Cys is used as a control (Fig. S1(a)). It is found that no color change can be induced by Al^{3+}, even at high Al^{3+} concentration up to 20.0 μM. However, when 50.0 mM of Cys is introduced (Fig. S1(b)), the color change of the detection system incubated with 2.0 or 20.0 μM of Al^{3+} is obvious. Because higher Cys concentration (100.0 or 150.0 mM) has no benefit to the sensitivity of the Al^{3+} detection system (Fig. S1(c) and (d)), 50.0 mM of Cys is chosen as the optimal condition in the following study.

The GSH-AgNPs dispersion without further addition of GSH is used as a control (Fig. S2(a)). As can be seen from the colorimetric detection images, compared with the control, the color change of the detection system (especially at 2.0 μM of Al^{3+}) is negligible when the GSH concentration is 0.6 mM (Fig. S2(b)), while it may become obvious when the GSH concentration is 6.0 mM (Fig. S2(c)), and become most clear at 10.0 mM of GSH concentration (Fig. S2(d)). That's because the GSH lower than 10.0 mM is not enough to completely cover the surface of the etched AgNPs and the complexation between Al^{3+} and GSH (on the surface of the etched AgNPs) cannot lead to obvious aggregation of the etched AgNPs. However, higher GSH concentration (13.0 or 20.0 mM) results in bad colorimetric detection effect (Fig. S2(e) and (f)). That is because the excess free GSH in solution complexes with Al^{3+} and then inhibits the interaction between Al^{3+} and GSH on the surface of the etched AgNPs. Therefore, the GSH concentration is fixed at 10.0 mM in the following experiments.

Influence of the pH value of the GSH-AgNPs-based detection system on the sensing effect of Al^{3+} is also investigated (Fig. S3). No obvious color change is found at pH 4.0, 7.0 and 9.0. However, at pH 6.0, the GSH-AgNPs-based detection system is very sensitive to Al^{3+} (the color changes obviously with introduction of 2.0 μM of Al^{3+}). Therefore, the pH value is fixed at 6.0 as an optimal condition in the following experiments.

3.2. Mechanism of the Al^{3+} detection system based on GSH-AgNPs

At the optimized conditions, the proposed new mechanism for Al^{3+} detection, i.e., aggregation of smaller etched AgNPRs (Scheme 1), is verified by TEM, EDS and DLS.

Fig. 1(a), (b), and (c) respectively shows the TEM images of GSH-AgNPs (control), GSH-AgNPs in the presence of Cys and GSH, and GSH-AgNPs incubated with 20.0 μM of Al^{3+} in the presence of Cys and GSH. It is found that the GSH-AgNPs are spherical and well-dispersed with particle size of around 10 nm (Fig. 1(a)). However, in the presence of Cys, the size of GSH-AgNPs decreases significantly due to the Cys etching effect (Fig. 1(b)). Furthermore, the smaller GSH-AgNPs etched by Cys aggregate to a great extent after being incubated with Al^{3+} (Figs. 1(c) and S4). Fig. 1(d), (e), and (f) respectively shows the EDS spectra of GSH-AgNPs, GSH-AgNPs in the presence of Cys and GSH, and GSH-AgNPs incubated with 20.0 μM of Al^{3+} in the presence of Cys and GSH. The EDS spectra confirm that GSH and Cys can be absorbed onto the surface of AgNPs due to the emergence of S element in the AgNPs (Fig. 1(d) and (e)), and the severe aggregation of the smaller etched GSH-AgNPs is induced by Al^{3+} because of the existence of Al^{3+} in the aggregated AgNPs (Fig. 1(f)). These results are in good agreement with our Al^{3+} detection strategy (Scheme 1).

Moreover, the DLS data reconfirm that the GSH-AgNPs etched by Cys aggregate to a great extent after being incubated with Al^{3+} (Fig. S5(a)). However, the DLS data also show that the mean particle size of GSH-AgNPs in the presence of Cys and GSH is larger than that of control without Cys and GSH (Fig. S5(a)). This result may be ascribed to the slight aggregation of AgNPs after Cys attack (Fig. S5(b)) because Cys is a worse stabilizer compared with GSH. Therefore, before Al^{3+} detection, an additional excess GSH needs to be introduced to the detection system to stabilize the etched AgNPs.

3.3. Selectivity of the Al^{3+} detection system based on GSH-AgNPs

The selectivity of the GSH-AgNPs-based detection system for Al^{3+} is evaluated by comparing with 14 kinds of metal ions (K^+, Mg^{2+}, Fe^{3+}, Co^{2+}, Mn^{2+}, Zn^{2+}, Cd^{2+}, Pb^{2+}, Ca^{2+}, Ba^{2+}, Cu^{2+}, Cr^{3+}, Hg^{2+} and Ni^{2+}) and 5 kinds of anions ($Cr_2O_7^{2-}$, SO_4^{2-}, $C_2O_4^{2-}$, PO_4^{3-} and CO_3^{2-}). Fig. 2 shows photographic image and UV–vis spectra of the GSH-AgNPs-based detection systems at the optimized conditions incubated with various metal ions or anions compared with Al^{3+}. As shown in the photographic image (Fig. 2(a)), the color of the detection system incubated with Al^{3+} changes from yellow to orange red, while no color change is induced by all other ions. Moreover, the UV–vis spectra (Fig. 2(b)) of the GSH-AgNPs-based detection system incubated with 20.0 μM of other metal ions or anions are similar with that in the absence of ions (blank), but very different with that incubated with 20.0 μM of Al^{3+} (red shift and intensity decrease). These results indicate that only Al^{3+} can trigger the aggregation of smaller etched AgNPs, and other metal ions or anions have no evident influence on the color and UV–vis spectra of the GSH-AgNP dispersion. Therefore, we can conclude that our proposed detection system exhibits excellent selectivity for Al^{3+} due to its new mechanism (i.e., aggregation of smaller etched AgNPs).

3.4. Sensitivity of the Al^{3+} detection system based on GSH-AgNPs

The colorimetric response and UV–vis spectra are also used to evaluate the sensitivity of our proposed GSH-AgNPs-based Al^{3+} detection system. Fig. 3 shows the photographic image and UV–vis spectra of the GSH-AgNPs-based detection systems at the optimized conditions containing various Al^{3+} concentrations from 0 to 20.0 μM. From Fig. 3(a), we can find that the color change of the Al^{3+} detection system become obvious when the Al^{3+} concentration is higher than 1.2 μM, which can be distinguished by the naked eyes. Therefore, the limit of detection (LOD) is 1.2 μM by the naked eyes.

From Fig. 3(b), we can find that the UV–vis spectrum shifts towards red and the absorption intensity decreases with increasing of Al^{3+}concentration. The absorption intensity of the detection system with 0.16 μM of Al^{3+} has a clear decrease compared with that of the blank without Al^{3+}. Therefore, the LOD is 0.16 μM by UV–vis spectrum.

The LOD of our Al^{3+} detection system by the naked eyes (1.2 μM) and UV–vis spectrum (0.16 μM) are both much lower than the national drinking water standards (200.0 μg/L, 7.4 μM), and very close to the lowest reported LOD by the naked eyes (1.0 μM) [25] and UV–vis spectrum (0.09 μM) [24] based on colorimetric detection systems of noble metal nanoparticles.

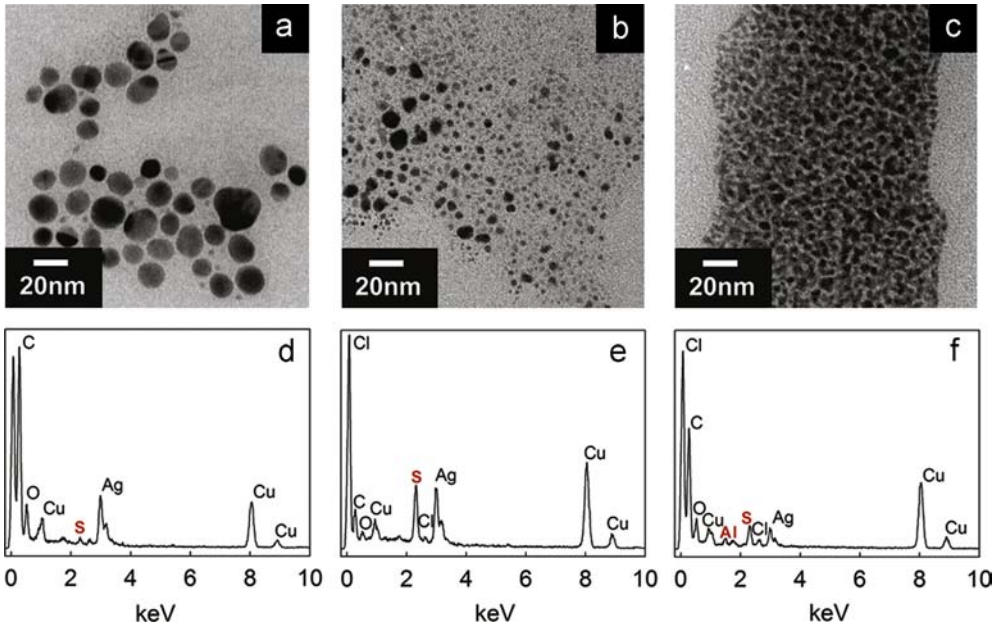

Fig. 1. TEM images of GSH-AgNPs without additional addition of Cys and GSH (control) (a), GSH-AgNPs-based detection system at the optimized conditions (b), GSH-AgNPs-based detection system at the optimized conditions incubated with 20.0 μM of Al^{3+} (c). (d), (e) and (f) EDS spectra of those samples used in (a), (b) and (c), respectively.

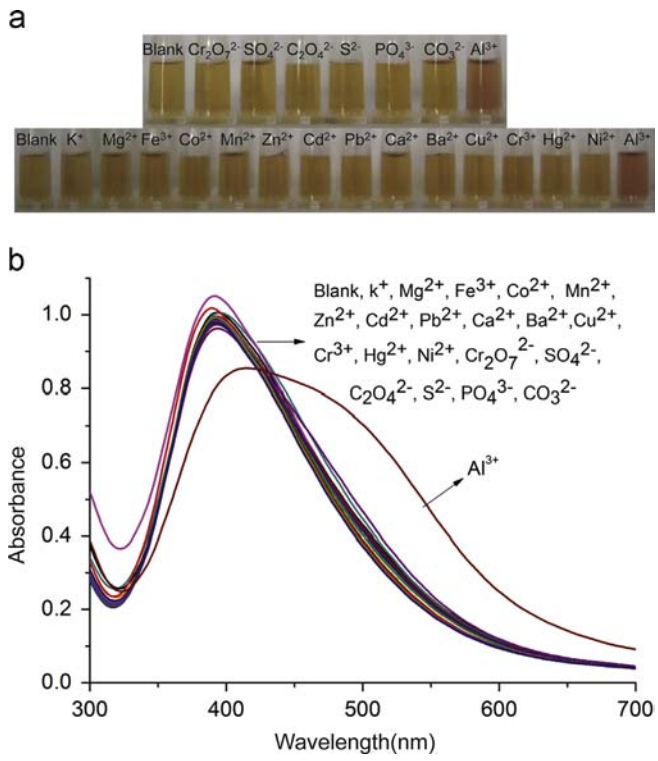

Fig. 2. Photographic image (a) and UV–vis spectra (b) of the GSH-AgNPs-based detection systems at the optimized conditions incubated with various metal ions or anions compared with Al^{3+}. The concentration of all ions used in this study is 20.0 μM.

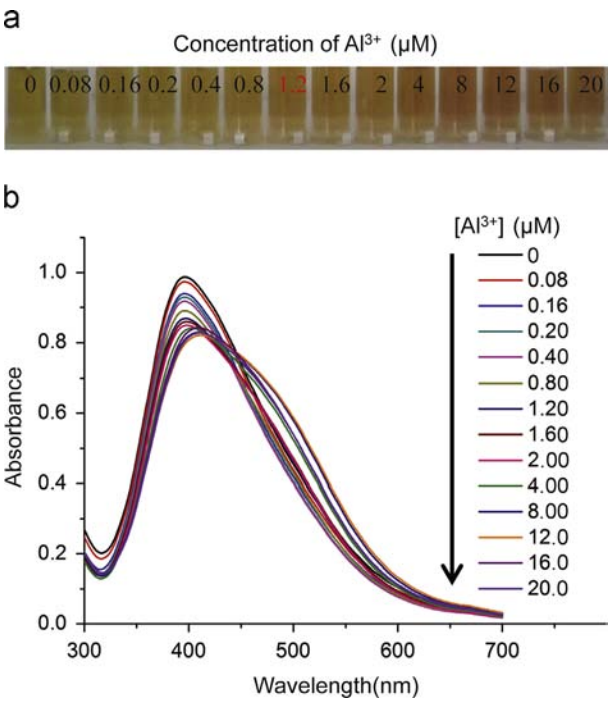

Fig. 3. Photographic image (a) and UV–vis spectra (b) of the GSH-AgNPs-based detection systems at the optimized conditions containing various Al^{3+} concentrations from 0 to 20.0 μM.

Furthermore, A_{412}/A_{395} of the GSH-AgNPs-based detection systems at the optimized conditions containing various Al^{3+} concentrations (calculated from the ratio of the absorbance at 412 nm to that at 395 nm) can be used for the quantitative analysis of Al^{3+}. The plot of A_{412}/A_{395} as a function of Al^{3+} concentration ranging from 0.08 to 20.0 μM is shown in Fig. 4. The inset plot shows the A_{412}/A_{395} versus different Al^{3+} concentrations ranging from 0.4 to 4.0 μM. We find it is a good linear relationship ($R^2=0.9924$) between the A_{412}/A_{395} and Al^{3+} concentrations ranging from 0.4 to 4.0 μM.

Consequently, the above results demonstrate that our GSH-AgNPs-based detection system based on new mechanism of aggregation of smaller etched AgNPs is applicable for rapid colorimetric detection and quantitative analysis of Al^{3+} with excellent selectivity and high sensitivity.

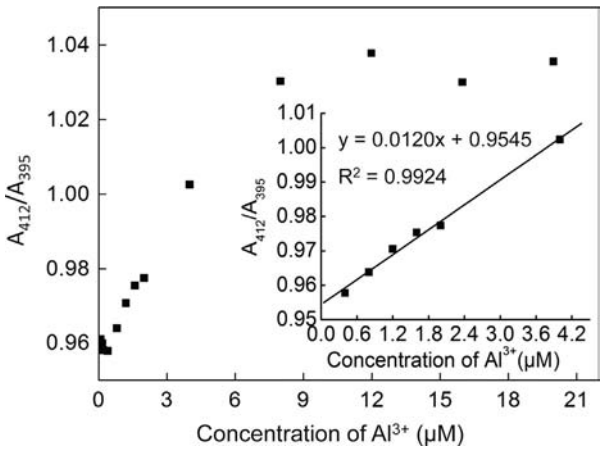

Fig. 4. Plot of A_{412}/A_{395} as a function of Al^{3+} concentration ranging from 0.08 to 20.0 μM. A_{412} and A_{395} are the absorbance of GSH-AgNPs-based detection systems (at the optimized conditions containing various Al^{3+} concentrations) at 412 nm and 395 nm, respectively. The inset plot shows the A_{412}/A_{395} versus different Al^{3+} concentration ranging from 0.4 to 4.0 μM.

Table 1
Determination of Al^{3+} in real water samples.

Samples	Al^{3+} added (μM)	Al^{3+} observed (μM) (Mean ± E, $n=3$)	ICP-AES observed (μM)
Tap water	0	0.10 ± 0.115	–
	0.5	0.73 ± 0.063	0.64
	1.0	1.19 ± 0.183	1.30

3.5. Detection of real water samples

In order to investigate the practical application of our Al^{3+} detection system, different concentrations of Al^{3+} were added into tap water and detected by our Al^{3+} detection system using the calibration curve in Fig. 4 as reported elsewhere [29,30]. The Al^{3+} concentration added into the tap water is 1.0 μM or 0.5 μM. The observed results using the calibration curve or ICP-MS are given in Table 1. We can find that the observed Al^{3+} concentrations by our calibration curve are very close to those added and those observed by ICP-MS. Moreover, we also test the effect of colorimetric method by naked eyes. The color change of the nanoparticle dispersions for detecting of real water samples (lake water) is in agreement with that of the control group and ICP result (Fig. S6 in Supporting Information). Consequently, our GSH-AgNPs-based detection system is applicable for Al^{3+} detection in the real environmental water samples.

4. Conclusions

A new facile and rapid Al^{3+} colorimetric detection system with high sensitivity and excellent selectivity based on GSH-AgNPs in the presence of Cys is proposed in this study. The new Al^{3+} detection mechanism of our GSH-AgNPs-based detection system, i.e., aggregation of smaller etched AgNPs, is verified by TEM, EDS and DLS. The GSH concentration, Cys concentration and pH value of the GSH-AgNPRs-based detection system are respectively optimized to be 10.0 mM, 5 mM and 6.0 according to the sensing effect of Al^{3+}. At the optimized conditions, our GSH-AgNPRs-based detection system has an excellent selectivity to Al^{3+} comparing with other metal ions (K^+, Mg^{2+}, Fe^{3+}, Co^{2+}, Mn^{2+}, Zn^{2+}, Cd^{2+}, Pb^{2+}, Ca^{2+}, Ba^{2+}, Cu^{2+}, Cr^{3+}, Hg^{2+} and Ni^{2+}) or anions ($Cr_2O_7^{2-}$, SO_4^{2-}, $C_2O_4^{2-}$, PO_4^{3-} and CO_3^{2-}) because only Al^{3+} can trigger the aggregation of smaller etched AgNPs resulting in obvious color change of the nanoparticle dispersion from yellow to reddish brown, and red shift and intensity decrease of the SPR absorption. The LOD of our Al^{3+} detection system by the naked eyes (1.2 μM) and UV–vis spectrum (0.16 μM) are both much lower than the national drinking water standards (200.0 μg/L, 7.4 μM). Furthermore, a good linear relationship ($R^2=0.9924$) is obtained between the A_{412}/A_{395} and Al^{3+} concentrations ranging from 0.4 to 4.0 μM, which indicates that our proposed Al^{3+} detection system can be used for the quantitative analysis of Al^{3+}. The detection results of real water samples indicate that this method can be used for real water detection.

Acknowledgments

This work was supported by the Program of National High-Tech Program (863 program, No. SS2012AA063202), the Program of Zhejiang Provincial Natural Science Foundation of China (Grant no. R5110230), the Natural Science Foundation of China (Grant no. 31128007), the Hundred Talents Program of Chinese Academy of Sciences and the Ningbo Science and Technology Bureau (Grants no. 2012A610174 and 2009B21005), the Projects Sponsored by the Scientific Research Foundation for the Returned Overseas Chinese Scholars, the States of Ministry of Human Resources & Social Security and the Ministry of Education, and Zhejiang Postdoctoral sustentation fund (Grant no. Bsh1201009).

Appendix A. Supporting information

Supplementary data associated with this article can be found in the online version at http://dx.doi.org/10.1016/j.talanta.2014.01.035.

References

[1] B. Dong, W.L. Sang, D.X. Jiang, J.M. Zhou, F.X. Kong, W. Hu, L.S. Wang, Chemosphere 47 (2002) 87–92.
[2] F.X. Kong, Y. Liu, W. Hu, P.P. Shen, C.L. Zhou, L.S. Wang, Chemosphere 40 (2000) 311–318.
[3] C. Struys-Ponsar, O. Guillard, P.V.B. de Aguilar, Exp. Neurol. 163 (2000) 157–164.
[4] S.R. Devi, Y. Yamamoto, H. Matsumoto, J. Inorg. Biochem. 97 (2003) 59–68.
[5] A. Campbell, K.N. Prasad, S.C. Bondy, Free Radic. Biol. Med. 26 (1999) 1166–1171.
[6] V.B. Gupta, S. Anitha, M.L. Hegde, L. Zecca, R.M. Garruto, R. Ravid, S.K. Shankar, R. Stein, P. Shanmugavelu, K.S.J. Rao, Cell. Mol. Life Sci. 62 (2005) 143–158.
[7] V. Riihimaki, H. Hanninen, R. Akila, T. Kovala, E. Kuosma, H. Paakkulainen, S. Valkonen, B. Engstrom, Scand. J. Work Environ. Health 26 (2000) 118–130.
[8] Y. Christen, Am. J. Clin. Nutr. 71 (2000) 621s–629s.
[9] S. Saito, T. Anada, S. Noshi, K. Akatsuka, Anal. Chem. 77 (2005) 5332–5338.
[10] P. Liang, L.H. Yang, B. Hu, Z.C. Jiang, Anal. Sci. 19 (2003) 1167–1171.
[11] N. Fujita, H. Kobayashi, T. Enami, N. Nagae, N. Charleston, Bunseki Kagaku 53 (2004) 17–23.
[12] H. Matsumiya, N. Iki, S. Miyano, Talanta 62 (2004) 337–342.
[13] E. Boisselier, D. Astruc, Chem. Soc. Rev. 38 (2009) 1759–1782.
[14] T.M. Tolaymat, A.M. El Badawy, A. Genaidy, K.G. Scheckel, T.P. Luxton, M. Suidan, Sci. Total Environ. 408 (2010) 999–1006.
[15] F.Q. Zhang, L.Y. Zeng, Y.J. Zhang, H.Y. Wang, A.G. Wu, Nanoscale 3 (2011) 2150–2154.
[16] Y. Yao, D.M. Tian, H.B. Li, ACS Appl. Mater. Interfaces 2 (2010) 684–690.
[17] F.Q. Zhang, L.Y. Zeng, C. Yang, J.W. Xin, H.Y. Wang, A.G. Wu, Analyst 136 (2011) 2825–2830.
[18] L.J. Miao, J.W. Xin, Z.Y. Shen, Y.J. Zhang, H.Y. Wang, A.G. Wu, Sens. Actuators B: Chem 176 (2013) 906–912.
[19] Y.X. Gao, J.W. Xin, Z.Y. Shen, W. Pan, X. Li, A.G. Wu, Sens. Actuators B: Chem 181 (2013) 288–293.
[20] J.W. Xin, L.J. Miao, S.G. Chen, A.G. Wu, Anal. Methods 4 (2012) 1259–1264.
[21] J.W. Xin, F.Q. Zhang, Y.X. Gao, Y.Y. Feng, S.G. Chen, A.G. Wu, Talanta 101 (2012) 122–127.
[22] Y.J. Zhang, Y.M. Leng, L.J. Miao, J.W. Xin, A.G. Wu, Dalton Trans. 42 (2013) 5485–5490.
[23] X.K. Li, J.N. Wang, L.L. Sun, Z.X. Wang, Chem. Commun. 46 (2010) 988–990.

[24] M. Zhang, Y.Q. Liu, B.C. Ye, Chem.—Eur. J. 18 (2012) 2507–2513.
[25] S. Chen, Y.M. Fang, Q. Xiao, J. Li, S.B. Li, H.J. Chen, J.J. Sun, H.H. Yang, Analyst 137 (2012) 2021–2023.
[26] X. Yuan, Y.Q. Tay, X.Y. Dou, Z.T. Luo, D.T. Leong, J.P. Xie, Anal. Chem. 85 (2012) 1913–1919.
[27] X. Wang, K. Li, X.D. Yang, L.L. Wang, R.F. Shen, J. Inorg. Biochem. 103 (2009) 657–665.
[28] H.B. Li, Z.M. Cui, C.P. Han, Sens. Actuators B: Chem. 143 (2009) 87–92.
[29] T.T. Lou, L.X. Chen, Z.P. Chen, Y.Q. Wang, L. Chen, J.H. Li, ACS Appl. Mater. Interfaces 3 (2011) 4215–4220.
[30] Y. Zhou, H. Zhao, C. Li, P. He, W.B. Peng, L.F. Yuan, L.X. Zeng, Y.J. He, Talanta 97 (2012) 331–335.